

# A Complete Relativistic Ionized Accretion Disc in Cygnus X–1

A.J. Young<sup>1,2</sup>, A.C. Fabian<sup>1</sup>, R.R. Ross<sup>3</sup> and Y. Tanaka<sup>4</sup>

<sup>1</sup>*Institute of Astronomy, Madingley Road, Cambridge CB3 0HA*

<sup>2</sup>*Present address Department of Astronomy, University of Maryland, College Park, MD 20742, USA*

<sup>3</sup>*Department of Physics, College of the Holy Cross, Worcester, MA 01610, USA*

<sup>4</sup>*Max-Planck-Institut für extraterrestrische Physik, D-85740 Garching, Germany*

26 October 2018

## ABSTRACT

The galactic black hole candidate Cygnus X–1 is observed to be in one of two X-ray spectral states; either the low/hard (low soft X-ray flux and a flat power law tail) or high/soft (high blackbody-like soft X-ray flux and a steep power law tail) state. The physical origin of these two states is unclear. We present here a model of an ionized accretion disc, the spectrum of which is blurred by relativistic effects, and fit it to the *ASCA*, *Ginga* and *EXOSAT* data of Cygnus X–1 in both spectral states. We confirm that relativistic blurring provides a much better fit to the low/hard state data and, contrary to some previous results, find the data of both states to be consistent with an ionized thin accretion disc with a reflected fraction of unity extending to the innermost stable circular orbit around the black hole. Our model is an alternative to those which, in the low/hard state, require the accretion disc to be truncated at a few tens of Schwarzschild radii, within which there is a Thomson-thin, hot accretion flow. We suggest a mechanism that may cause the changes in spectral state.

**Key words:** accretion, accretion discs — binaries: close — black hole physics — stars: individual (Cygnus X–1) — X-ray: general — X-ray: stars

## 1 INTRODUCTION

Cygnus X–1 (Cyg X–1) is one of the brightest and best studied X-ray sources in the sky. It was the first source to be identified with a binary system in which the X-ray emission arises through accretion onto a compact object. (See e.g. Tanaka & Lewin (1995) for a review of black hole binaries). It is at a distance of  $\sim 2$  kpc (Massey et al. 1995) and consists of a supergiant star and a compact object, with an orbital period of 5.6 days. The mass of the unseen companion is significantly greater than  $5M_{\odot}$  (Dolan 1992) suggesting that it is a black hole. The high energy emission results from focused wind accretion from the supergiant (Gies & Bolton 1986) that is almost filling its Roche lobe. The X-ray flux varies on all timescales from milliseconds to months although most of its time is spent in the so-called low or hard state (the ‘low/hard’ state) characterized by a low soft X-ray flux and strong hard X-ray flux. Occasionally Cyg X–1 makes a transition from the low/hard state to the high/soft state which is characterized by a larger soft X-ray flux (by a factor of  $\sim 10$ ) and weaker hard X-ray flux.

The spectrum in the low/hard state above a few keV is typically a power law of photon index  $\Gamma \sim 1.6$ – $1.8$  and a Compton reflection component above about 10 keV (Done

et al. 1992; Ebisawa et al 1996) with a high-energy cut-off above  $\sim 100$  keV. There is evidence of complicated iron absorption and emission features around 6–7 keV (Barr, White & Page 1985; Marshall et al. 1993; Ebisawa et al. 1996).

In the high/soft state the spectrum is dominated by a soft blackbody-like component peaking around 1 keV with a power law tail of photon index  $\Gamma \approx 2.5$  (Gierliński et al. 1999).

It has been suggested that the different spectral states are due to a qualitative change in the accretion flow (see e.g. Gierliński et al. 1997; Esin et al. 1998; Poutanen & Coppi 1998; Done & Zycki 1999). In the high/soft state there is a ‘standard’ accretion disc extending in to the innermost stable circular orbit around the black hole, and in the low/hard state the region within a few 10s of Schwarzschild radii becomes a geometrically thick, optically thin, radiatively inefficient advective flow (see also Nowak et al. 1999). The evidence for this is that in the low/hard state the reflected fraction appears to be low, which is consistent with the innermost parts of the accretion disc being missing, or at least Thomson thin. The change between spectral states occurs with a small change in bolometric luminosity ( $\sim 50$  per cent) and no change in 1.3 – 200 keV luminosity to within  $\sim 15$  per cent (Zhang et al. 1997).

No.	Date	Observation	State
1	1993 Oct	<i>ASCA</i> GIS	Low/hard
3	1993 Nov 11	<i>ASCA</i> GIS	Low/hard
4	1993 Nov 12	<i>ASCA</i> GIS	Low/hard
5	1993 Nov	<i>ASCA</i> SIS	Low/hard
6	1994 Nov	<i>ASCA</i> GIS, no.1	Low/hard
7	1994 Nov	<i>ASCA</i> GIS, no.2	Low/hard
8	1994 Nov	<i>ASCA</i> GIS, no.3	Low/hard
9	1994 Nov	<i>ASCA</i> GIS, no.4	Low/hard
10	1994 Nov	<i>ASCA</i> GIS, no.5	Low/hard
a	1991 Jun 6	<i>Ginga</i> no. 2	Low/hard
b	1996 May	<i>ASCA</i> SIS	High/soft
E08	1984 Jul 9	<i>EXOSAT</i> GSPC	Low/hard
E09	1985 Sep 14	<i>EXOSAT</i> GSPC	Low/hard
E10	1985 Aug 12	<i>EXOSAT</i> GSPC	Low/hard
E13	1984 Nov 2	<i>EXOSAT</i> GSPC	Low/hard
E14	1984 Nov 2	<i>EXOSAT</i> GSPC	Low/hard

**Table 1.** Data sets used. The data set numbers 1 and 3–10 correspond to those of Ebisawa et al. (1996), and those prefixed by ‘E’ correspond to those of Done et al. (1992).

In this paper we investigate an alternative model in which the low inferred reflected fraction is a result of the ionization state of the accretion disc. A highly ionized disc may be an almost perfect reflector with weak reflection features (as compared to cold reflection) and hence may lead to an underestimate of the reflected fraction (Ross, Fabian & Young 1999; Ross, Fabian & Brandt 1996; Ross & Fabian 1993; Nayakshin, Kazanas & Kallman 2000). The attraction of this model is that it does not require the nature of the accretion flow to change qualitatively between the spectral states; a change which is observed to occur with little variation in bolometric luminosity as observed. It is just a change in density at the surface of the disc.

Previous conclusions that the disc cannot be significantly ionized have been based on the absence of a strong photoelectric absorption edge at 8 keV. In the case of an ionized disc absorption and emission may occur at significant Thomson depths ( $\tau_T \gtrsim 1$ ) and sharp features are blurred due to Compton scattering. See e.g. Fig. 7 of Ross, Fabian & Young (1999).

In view of the extremely rapid continuum variability of Cyg X–1 we may also expect its spectrum to change rapidly. The spectra that we fit are necessarily time averaged since a typical observation will last for millions of dynamical timescales.

## 2 DATA AND MODEL

### 2.1 Data

We use *ASCA* SIS, *ASCA* GIS, *EXOSAT* and *Ginga* data of Cyg X–1 in the low/hard state and *ASCA* SIS data of Cyg X–1 in the high/soft state. We do not use the *ASCA* 93 Oct data of the low/hard state since this was taken when the satellite was in daytime (Ebisawa et al. 1996). The data used are summarized in Table 1.

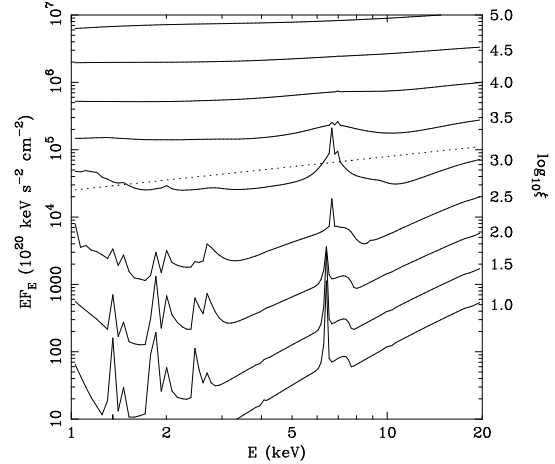


**Figure 1.** Reflection spectra from a slab of gas illuminated by an X-ray power law of photon index  $\Gamma = 1.6$ , solar iron abundance and various values of the ionization parameter  $\xi$ . The lowest solid line is for  $\log \xi = 1$ , and  $\log \xi$  increases upwards to  $\log \xi = 5$  in steps of 0.5. The dotted line is a representative illuminating power law, in this instance the  $\log \xi = 3$  case.

### 2.2 Rest frame reflection spectra

The accretion disc model is based on the X-ray reflection spectra from ionized slabs of gas calculated by Ross, Fabian & Young (1999) and Ross & Fabian (1993). The reflection spectrum resulting from the illumination of a slab of gas by an X-ray power law of photon index  $\Gamma$  depends primarily on the ionization parameter  $\xi$ , defined as the ratio of flux and density,

$$\xi = \frac{4\pi F_x}{n_H}$$

where  $F_x$  is the illuminating X-ray flux (0.01–100 keV) and  $n_H$  is the hydrogen number density. Fig. 1 shows reflection spectra calculated for solar iron abundance, a photon index of 1.6 and a range of ionization parameters,  $\log \xi = 1 - 5$  in steps of 0.5.

For very low ionization parameters the most prominent feature of the reflected spectrum is the iron fluorescence line at 6.4 keV. In neutral gas both oxygen and iron are strong absorbers but the absorption above and below the iron edge is so strong that the change in observed flux across the edge is small, particularly if the primary continuum is also observed. This absorption also tends to harden the spectrum as compared to the illuminating power-law.

As the X-ray illumination of the slab becomes more intense the matter becomes more highly ionized. This reduces the effects of absorption progressively from lower to higher energies. An important signature of ionized reflection is a strong iron edge. As much of the oxygen becomes completely ionized the edge becomes more prominent as the absorption below it is reduced. As the outer layers of the slab become completely ionized fluorescent photons are produced deeper in the slab and are Compton scattered on leaving the slab resulting in broad and blended emission and absorption features, e.g. the case of  $\xi = 10^3$  in Fig. 1. The narrow line cores are from those line photons that escape without scattering or are generated closer to the surface. For an extremely highly

ionization parameter  $\xi = 10^5$  the reflection spectrum is almost indistinguishable from the illuminating continuum.

### 2.3 Simple accretion disc model

Initially we consider a model of a non-relativistic accretion disc with a single ionization parameter  $\xi$ . This consists of two components; the primary X-ray source which we assume to be a power law of photon index  $\Gamma$  and the reflected spectrum corresponding to some fraction of these X-rays being Compton scattered by the disc into our line of sight.

We have computed a grid of reflection spectra for a range of photon indices, ionization parameters and iron abundances, and subsequently converted to an XSPEC ‘tablemodel’. XSPEC is the spectral fitting code commonly used by X-ray astronomers. The reflection spectra in the tablemodel have been scaled so that, in XSPEC, a reflection spectrum plus power law of the same photon index has a corresponding reflected fraction equal to the ratio of the normalization of the reflected spectrum to the power law. We have considered ionization parameters in the range  $\xi = 10^1$ – $10^5$  (up to  $\xi = 10^6$  in the high/soft case) and iron abundances in the range 1–3×solar.

### 2.4 Relativistic blurring

The accretion disc is deep in the potential well of the black hole and subject to strong Doppler, transverse Doppler and gravitational redshifting effects. These will smear out the sharp features in the spectrum and blend the emission and absorption features together. The detection of such an effect in the spectrum of Cyg X-1 in the low/hard state has been reported by Done & Zycki (1999) but with quite different parameters to those reported here. We compute this in XSPEC by convolving the spectrum with a blurring kernel taken from the DISKLINE model for an accretion disc around a Schwarzschild black hole (Fabian et al. 1989). Special care needs to be taken when using this approach in XSPEC since it requires the model to be evaluated outside the energy range of the data. This is discussed in Appendix A.

The parameters of the blurring model define the inner and outer radii of our accretion disc. The outer radius is fixed at  $1000r_g = 1000GM/c^2$ , and the inner radius  $r_{\text{in}}$  must be  $\geq 6r_g$  ( $6r_g = 6GM/c^2 = 3R_S$ , where  $R_S$  is the Schwarzschild radius, and is the location of the innermost stable circular orbit around a Schwarzschild black hole). The precise value of the outer radius has little impact on the results we present here. The ‘radial emissivity profile’ parameter required for the DISKLINE kernel is set to  $(1 - \sqrt{6/r_g})/r_g^3$ .

### 2.5 A more realistic disc model

We shall find that some of the data sets require the use of a more sophisticated model. In the future it will be useful to construct a proper model that accounts for the radial variation of ionization parameter in more detail, but for the time being we use the prescription described below.

The accretion disc is divided into two zones, an ‘inner’ region which will have a relatively high ionization parameter, and an ‘outer’ region with a lower ionization parameter. The inner and outer regions are convolved with DISKLINE

kernels extending between  $6r_g \rightarrow r_{\text{trans}}$  and  $r_{\text{trans}} \rightarrow 1000r_g$  respectively, where  $r_{\text{trans}}$  represents the radius of the transition between high and low ionization zones. The relative contribution to the reflection from regions  $r < r_{\text{trans}}$  and  $r > r_{\text{trans}}$  are calculated to agree with the Page & Thorne (1974) radial emissivity law. From a practical point of view, fitting the data using XSPEC, this achieved iteratively, i) fitting the data, ii) fixing  $r_{\text{trans}}$  at the appropriate value given the relative contribution to the reflection from the two regions, iii) repeating until a self-consistent fit is achieved. Very few iterations were required. The error in determining  $r_{\text{trans}}$  is quite small as an uncertainty of  $\sim 10$  per cent in the ratio of fluxes would correspond to an error of  $\pm 2r_g$  in  $r_{\text{trans}}$ . This represents a realistic model of an accretion disc with a sharp transition from high to low ionization state. Whether such an abrupt transition is *required* will be investigated later.

## 3 FITS TO ASCA SIS DATA

In this section we consider various fits to the ASCA SIS data of Cyg X-1 in both the high/soft and low/hard states. We are mainly interested in fitting the data between 4–10 keV since this is where most of the ionized reflection features are expected to lie. It is also uncertain as to whether the primary X-ray continuum is actually a power-law over the entire ASCA energy range.

### 3.1 Simple disc model

#### 3.1.1 Low/hard state

We begin by fitting a non-relativistically blurred ionized disc model to the 4–10 keV ASCA SIS data of the low/hard state. In these fits the iron abundance has been fixed at twice solar, the best fitting value suggested by Done & Zycki (1999). Such a model is not able to give a good fit to the data but it is interesting to consider a plot of  $\chi^2$  against  $\xi$  shown in Fig. 2. The solid curve shows the quality of fit with the reflected fraction  $f$  frozen at 1, i.e. with the disc subtending  $2\pi$  sr of the sky as seen by the X-ray source. There are two local minima, one at  $\xi = 10^2$  and the other around  $\xi = 10^4$ . The best fitting solution obtained will depend upon the initial value of  $\xi$ , the separatrix being at approximately  $\xi = 10^3$ . The horizontal dotted line shows the  $\chi^2$  value for a reflected fraction of 0, and the dashed line shows the values with the reflected fraction free parameter.

In the case of a low ionization parameter  $\xi = 10$  a fit with a reflected fraction of 1 is significantly worse than that of just a power law. A much smaller reflected fraction  $f = 0.07$  provides a better fit. For an ionization parameter of  $\xi = 10^2$  at the first minima in  $\chi^2$  we again find a low reflected fraction is preferred, with  $f = 0.55$ . At the second minima  $\xi = 10^{3.8}$ , however, we find the best fitting reflected fraction to be  $f = 1.07$ . Table 2 summarizes the results of these provisional fits. The values of the photon index  $\Gamma$  are consistent with the results of Gierliński et al. (1997).

To summarize, we have found two distinct solutions, one preferring a low ionization parameter and low reflected fraction, the other preferring high ionization parameter and

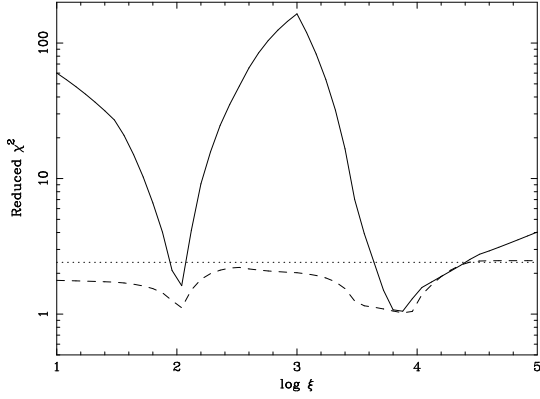


**Figure 2.** (Low/hard). Results of fitting the ionized disc model, without relativistic blurring or additional spectral components, to the 93 Nov *ASCA* data of Cyg X-1 in the low/hard state. The solid curve shows the reduced  $\chi^2$  value for a reflected fraction of 1, the dotted line for a reflected fraction of 0 and the dashed line for the reflected fraction being a free parameter. When the reflected fraction is a free parameter it has been fitted for at each value of  $\xi$ .

Data set	State	$\log \xi$	$\Gamma$	$^b f$	$\chi^2/\text{dof}$
5	low/hard	1.0 <sup>a</sup>	1.57	0.07	128/76
5	low/hard	2.0 <sup>a</sup>	1.65	0.55	78/76
5	low/hard	3.8 <sup>a</sup>	1.68	1.07	75/76
5	low/hard	5.0 <sup>a</sup>	1.54	0.00	178/76
b	high/soft	1.0 <sup>a</sup>	2.36	0.17	57/37
b	high/soft	2.4 <sup>a</sup>	2.47	1.14	33/37
b	high/soft	5.1 <sup>a</sup>	2.32	1.13	37/37
b	high/soft	6.0 <sup>a</sup>	2.21	162	70/37

<sup>a</sup> frozen

<sup>b</sup> reflected fraction ( $2\pi$  sr)

**Table 2.** Fit statistics for an ionized accretion disc model, without relativistic blurring or additional spectral components. Although some of these fits appear to be statistically acceptable some show systematic residuals at the expected energies of line and edge features.

a high reflected fraction. We shall investigate both of these with a more realistic physical model.

### 3.1.2 High/soft state

Similar results are obtained for the high/soft state, where we have considered ionization parameters up to  $\xi = 10^6$ , as shown in Fig. 3. The location of the minima have changed to  $\xi = 10^{2.5}$  and  $\xi = 10^5$ . Table 2 also shows the results of these provisional fits. A low reflected fraction seems to be preferred for an unionized disc although a fraction closer to 1 is acceptable in the case of the disc being ionized. The values of the photon indices  $\Gamma$  are consistent with those found by Gierliński et al. (1999) when they include *OSSE*  $\gamma$ -ray observations.

## 3.2 Relativistic blurring

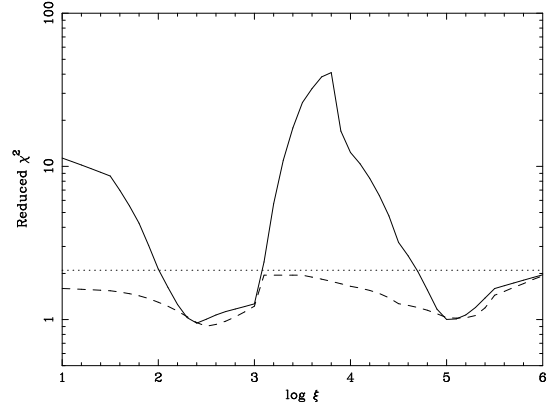


**Figure 3.** (High/soft). Results of fitting the ionized disc model, without relativistic blurring or additional spectral components, to the *ASCA* data of Cyg X-1 in the high/soft state. The solid curve shows the reduced  $\chi^2$  value for a reflected fraction of 1, the dotted line for a reflected fraction of 0 and the dashed line for the reflected fraction being a free parameter. When the reflected fraction is a free parameter it has been fitted for at each value of  $\xi$ .

### 3.2.1 Low/hard state

We fit the *ASCA* data of the low/hard state between 4–10 keV with the ionized disc model convolved with the relativistic blurring model described above. The reflected fraction is fixed to 1 and the iron abundance to twice solar. Without relativistic blurring we found there to be two local minima in  $\chi^2$  around  $\xi = 10^2$  and  $\xi = 10^{3.8}$ . We first consider an accretion disc with the inner radius fixed at  $r_{\text{in}} = 6r_g$ , the outer radius fixed at  $50r_g$  and the inclination a free parameter. This improves the quality of fit significantly around  $\xi = 10^2$  and only slightly around  $\xi = 10^{3.8}$  to such an extent that the  $\xi = 10^2$  solution is now (only just) favoured. If we now allow the inner disc radius to be a free parameter we get a better fit for very low values of the ionization parameter but almost no change at the best fitting values. These results are shown in Fig. 4.

### 3.2.2 High/soft state

In contrast to the low/hard state Fig. 5 shows that relativistic blurring does not significantly improve the quality of the best fits, and it is possible to achieve an equally good fit with or without blurring, with ionization parameters of  $\xi = 10^{2.5}$  and  $\xi = 10^5$ . In the case of cold reflection, however, blurring does significantly improve the quality of fit.

## 4 FITS TO THE *ASCA*, *GINGA* AND *EXOSAT* DATA

When we fit the *ASCA* GIS data we find that a satisfactory fit cannot be achieved with a disc that has a single ionization parameter. This is not too surprising since the the models is extremely simplified, and the GIS data have a better spectral resolution than the SIS data at higher energies, and provide a more stringent test for theoretical models. A model in which the disc is divided into two regions, each

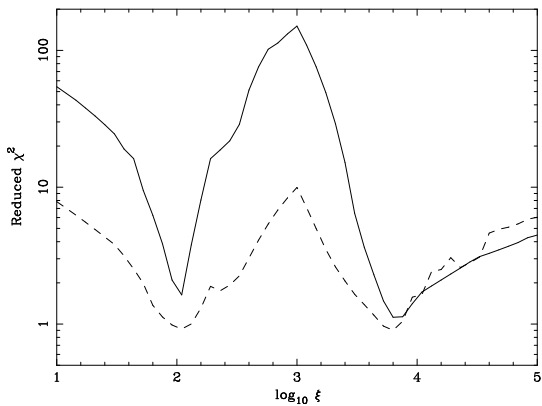


**Figure 4.** (Low/hard). Results of fitting the relativistically blurred ionized disc model to the 93 Nov *ASCA* data of Cyg X-1 in the low/hard state. The reflected fraction has been fixed at 1. The solid curve shows the fit without relativistic blurring, and the dashed line shows the improvement with blurring from an accretion disc spanning  $6 - 50r_g$ . The inclination angle is a free parameter, fitted for at each value of  $\xi$ .

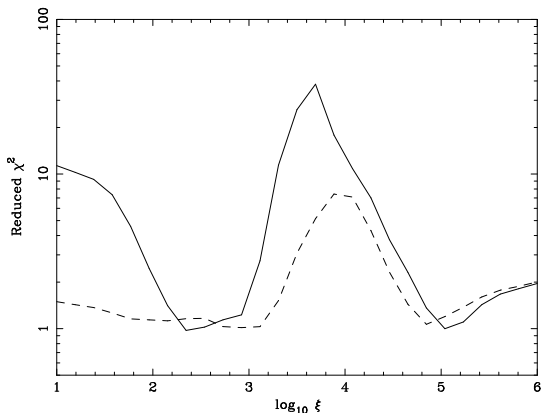


**Figure 5.** (High/Soft). Results of fitting the relativistically blurred ionized disc model to the 93 Nov *ASCA* data of Cyg X-1 in the high/soft state. The reflected fraction has been fixed at 1. The solid curve shows the fit without relativistic blurring, and the dashed curve shows the change when blurring from an accretion disc spanning  $6 - 50r_g$  is included.

with a different ionization parameter, does provide a satisfactory fit to the data. This is not a perfect model, but it is more realistic than one in which there is a single ionization parameter. The details of the model are discussed in section 2.5. To fit the data with such a model we initially allow  $r_{\text{trans}}$  and the relative normalizations of the inner and outer components to be free parameters. Fitting this model to the data gives the approximate relative normalization of the inner and outer components allowing the corresponding  $r_{\text{trans}}$  to be computed.  $r_{\text{trans}}$  is then frozen at this value and the data are fit again. We check the relative fluxes of the two components are still consistent with the  $r_{\text{trans}}$ . This ensures that each of the components is blurred appropriately.

The results of fitting this model to the *ASCA* SIS and GIS, *Ginga* and *EXOSAT* data are summarized in table 4. The reduced  $\chi^2$  values of the fits to the *ASCA* GIS data are comparable to those found by Ebisawa et al. (1996) and Done & Życki (1999). Overall this model is able to provide

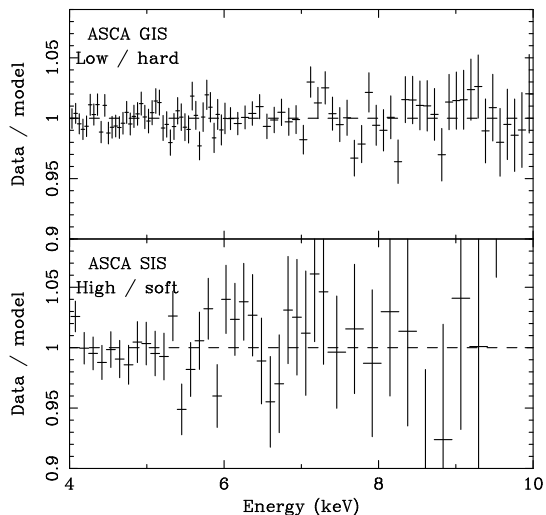


**Figure 6.** Typical ratio plots of good fits to the *ASCA* data of Cyg X-1 in both the low/hard and high/soft state.

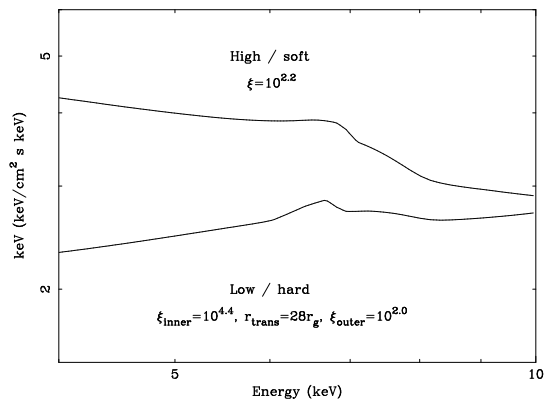


**Figure 7.** Two models that provide good fits to the *ASCA* data of Cyg X-1 in the high/soft and low/hard states.

a good fit to the available data. The preferred inclination angles tend to be small which is in reasonable agreement with the optical studies of Gies & Bolton (1986) in which the most probable inclination angle is  $28^\circ - 38^\circ$ .

The low/hard state may be characterized by an accretion disk in which the inner region within  $\sim 13$  Schwarzschild radii is highly ionized,  $\xi \sim 10^4$ , and outside of which the disk is less highly ionized,  $\xi \sim 10^2$ . In the high/soft state we have only fitted one data set, but that is consistent with a relatively cool accretion disk. In all cases the accretion disk extends in to the innermost stable orbit and has a reflection fraction of unity. Fig. 6 shows typical fits to the *ASCA* GIS data of the low/hard state and *ASCA* SIS data of the high/soft state. The corresponding models are shown in Fig. 7

Note that in these fits we have not added any contribution to the spectrum from thermal disk emission (which will have a small effect on these fits since we are fitting above 4 keV), or any contribution to the iron line from reflection off the companion star. This would consist of a narrow iron line at 6.4 keV of low equivalent width. Either of these measures could improve the quality of fit listed in table 4.

Data set	<sup>a</sup> PL $\Gamma$	<sup>b</sup> $\log_{10} \xi_{\text{inner}}$	$r_{\text{trans}} (r_g)$	$\log_{10} \xi_{\text{outer}}$	<sup>c</sup> inc	$\chi^2$	/	d.o.f.
1	1.79	$4.4^{+0.1}_{-0.2}$	26	$1.8^{+0.1}_{-0.2}$	33	111	/	85
3	1.75	$4.4^{+0.1}_{-0.1}$	28	$2.0^{+0.1}_{-0.0}$	11	75	/	81
4	1.61	$5.0_{-0.2}$	22	$2.0^{+0.2}_{-0.0}$	8	129	/	81
5	1.59	$3.9^{+0.1}_{-0.0}$	26	$2.0^{+0.1}_{-0.1}$	7	66	/	77
6	1.57	$4.4^{+0.1}_{-0.1}$	30	$1.9^{+0.1}_{-0.0}$	0	100	/	84
7	1.49	n/a	6	$2.0^{+0.0}_{-0.0}$	$41^{+5}_{-3}$	77	/	87
8	1.52	$4.3^{+0.1}_{-0.1}$	36	$2.0^{+0.0}_{-0.2}$	4	115	/	85
9	1.50	$2.3^{+0.4}_{-0.8}$	36	$1.6^{+0.2}_{-0.6}$	1	92	/	85
10	1.46	$5.0^{+}_{-0.3}$	22	$2.0^{+0.1}_{-0.1}$	7	103	/	85
a	1.58	$4.5^{+0.5}_{-0.3}$	20	$2.0^{+0.3}_{-0.4}$	1	4	/	13
E08	1.65	$4.4^{+0.4}_{-0.3}$	30	$1.8^{+0.1}_{-0.2}$	23	57	/	80
E09	1.50	$5.0_{-0.7}$	12	$1.9^{+0.1}_{-0.4}$	20	81	/	67
E10	1.44	$4.3^{+0.2}_{-0.1}$	43	$1.7^{+0.2}_{-0.3}$	20	53	/	76
E13	1.68	$4.7^{+0.3}_{-0.3}$	21	$1.7^{+0.2}_{-0.2}$	38	143	/	152
E14	1.61	$4.3^{+0.2}_{-0.1}$	24	$2.0^{+0.0}_{-0.0}$	20	64	/	75
b	2.46	n/a	6	$2.2^{+0.2}_{-0.2}$	13	36	/	36

<sup>a</sup> power law photon index  $\Gamma$

<sup>b</sup> 5.0 is the upper limit for this parameter

<sup>c</sup> accretion disc inclination angle

**Table 3.** Fit statistics for our model of a complete ( $6r_g \rightarrow 1000r_g$ ) relativistically smeared ionized accretion disc with a reflected fraction of unity. The low/hard state data are above the separating line, the high/soft state data below.

## 5 TRANSITION REGION

So far we have assumed a sharp transition between the high ionization inner zone and the lower ionization outer zone. It is important to try and quantify the sharpness of this transition. Some models such as those of Ross & Fabian (1993) predict that as the ionization parameter decreases outwards there should be a zone in which H-like and He-like iron fluorescence is observed. This has twice the fluorescence yield of neutral iron, and produces strong lines at 6.67 keV and 6.97 keV. Other models, such as those of Nayakshin et al. (2000) and Nayakshin (2000) predict the strength of the iron line to decrease monotonically with radius, i.e. it is not necessary to have an annulus in which strong H-like and He-like iron fluorescence is produced.

To investigate whether an intermediate zone in which H-like and He-like iron are produced is consistent with the data we modified the ionized disc model as follows. An extra zone was introduced of width  $\Delta r$ , with an ionization parameter fixed so that the reflected spectrum had H-like and He-like iron emission, and the normalization fixed so that the ratio of model flux in  $6r_g \rightarrow r_{\text{trans}}$  to that in  $r_{\text{trans}} \rightarrow r_{\text{trans}} + \Delta r$  is equal to that expected for a standard accretion disc. Fits were then performed to see how the best fitting  $\chi^2$  values changed with  $\Delta r$ . For data set 3 (*ASCA* GIS) the results are shown in Fig. 8.

The introduction of a zone of H-like and He-like iron makes the fit progressively worse as the width of the zone increases. The overall best fit is achieved without such a zone, i.e. with a sharp transition. With the present quality of data, however, acceptable fits are obtained with a zone of reasonable width,  $\sim$  few  $r_g$ , and we cannot rule out a gradual change in ionization parameter.

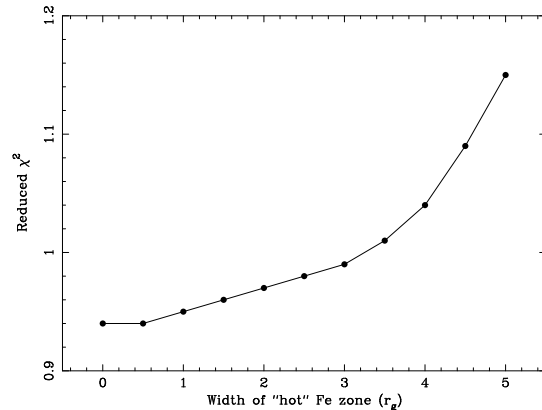


**Figure 8.** Change in  $\chi^2$  of fit to data set 3 (*ASCA* GIS) with the introduction of a transition zone of width  $\Delta r$  in which the reflected spectrum has H-like and He-like iron lines. The best overall fit is achieved with a sharp transition (i.e.  $\Delta r = 0$ ) but the data are not of sufficient quality to rule out a gradual transition.

## 6 DISCUSSION

We have shown that a relativistically blurred accretion disc with two ionization states is able to fit the X-ray data of Cyg X-1. The disc may extend in to the innermost stable orbit around the black hole, and have a reflected fraction of 1. We present this model as an alternative to those in which, in the low/hard state, the outer accretion disc is not ionized and extends in to a few 10s of Schwarzschild radii, within which the accretion flow becomes geometrically thick, optically thin and radiatively inefficient. One attraction of our model is that the accretion flow need not change qualitatively between the two spectral states of Cyg X-1; it just

State	$^a \xi$	$^b f_c$	$^c f$	$^d \Gamma$
Low/hard	High	$\gtrsim 0.4$	Low	Low
High/soft	Low	$\lesssim 0.1$	High	High

<sup>a</sup> ionization parameter

<sup>b</sup> fraction of accretion power dissipated in the corona

<sup>c</sup> inferred reflected fraction

<sup>d</sup> observed photon index

**Table 4.** Model predictions; see discussion

requires a change in the surface density of the disc. Fig. 7 shows two representative fits to the data.

It is also clear that, in the low/hard state, relativistic blurring of the disc spectra results in a significant improvement in the quality of fit.

It should be noted that our model is simplified in that the accretion disc is assumed to have two ionization zones. With the present data we are unable to investigate the radial (or indeed azimuthal) dependence of the ionization parameter in sufficient detail.

## 6.1 State changes in Cyg X-1

We now discuss a possible accretion disc model to explain the differing spectral properties of Cyg X-1 in the low/hard and high/soft states. Most of the time Cyg X-1 is in the low/hard state and it makes occasional transitions to the high/soft state. The mechanism for this transition is at present poorly understood. We propose a model in which the state change is due to a change in the ratio,  $f_c$ , of accretion power dissipated in the corona to that dissipated in the disc.

If most of the accretion power is dissipated in the disc,  $f_c \lesssim 0.1$ , we expect significant thermal blackbody emission from the disc. There are then many UV seed photons to be inverse Compton scattered in the corona and the X-ray spectrum will be relatively soft. If on the other hand significant power is dissipated in the corona,  $f_c \gtrsim 0.4$ , we expect the blackbody emission to be reduced. The seed-photon-starved corona will produce a harder spectrum. A combination of factors may then give rise to the observed behaviour of the ionization parameter. Firstly, a larger fraction of accretion power being dissipated in the corona provides increased hard X-ray illumination of the disc, and hence a larger value of  $\xi$  (note that the bolometric luminosity remains constant with changing  $f_c$  but the ratio of hard to soft flux does change). Secondly, the inverse Compton temperature is much higher for a hard illuminating spectrum than a soft one, and if the outermost layers of the disc heat up to the Compton temperature (e.g. see Róžańska 1999; Nayakshin, Kazanas & Kallman 2000) this will be important in determining the observed value of  $\xi$ . A final possibility is that the density of the surface layers of the disc changes between spectral states, with the low/hard state having a lower surface density (giving rise to a higher value of  $\xi$ ) than the high/soft state. Table 4 summarizes the expected properties of this simple model.

We also note that the predictions of changing spectral slope are consistent with the calculations of Coppi (1999) in which an increase in the soft flux coupled with a reduction

of the hard flux leads to an increase in the photon index of the continuum, i.e. a softer spectrum.

Our simple model is also consistent with the observational results of Zdziarski, Lubiński & Smith (1999) whereby the inferred (cold) reflected fraction is correlated with the observed photon index. The correlation is almost linear ranging from a reflected fraction of 0 with a photon index of  $\Gamma = 1.6$  up to a reflected fraction of 2 with a photon index of  $\Gamma = 2.2$ , with some scatter. This correlation is also seen within individual objects whose photon indices and reflected fractions change with time. We predict that a softer spectrum (high photon index) should have a lower value of the ionization parameter and hence most of the disc may produce a cold line resulting in a large inferred reflected fraction. In the case of a harder spectrum (low photon index) we predict a higher value of the ionization parameter and the spectrum will be that of an ionized disc as discussed above. This may result in the inferred reflected fraction being lower. Another model that is able to reproduce this correlation is that of Beloborodov (1999) in which the X-ray sources move away from the disc at mildly relativistic speeds.

Further detailed calculations are, of course, required to investigate this model properly. It is not clear how Cyg X-1, and other BHC, remain ‘locked’ into their spectral states when the dynamical timescale is so short.

## 6.2 Future observations and theory

Future observations with higher spectral resolution will provide much more stringent tests of the accretion disc models for Cyg X-1 and other BHC. At present, even with the *ASCA* data, we are unable to place strong constraints on the parameter space of our model (e.g. inner disc radius, reflected fraction) as our statistics are not good enough.

This model is also applicable to other black hole candidates and we hope to investigate these in the future. More complete models that account for the detailed ionization structure of the accretion disc as a function of radius need to be computed.

## 7 ACKNOWLEDGEMENTS

We thank Ken Ebisawa for the *ASCA* and *Ginga* data of Cyg X-1 in the low/hard state, and Keith Arnaud for advice on solving our convolution problem. We would also like to thank the referee P. T. Życki for helpful comments. AJY thanks PPARC for support. ACF thanks the Royal Society.

## REFERENCES

- Barr P., White N.E., Page C.G., 1985, MNRAS, 216, 65
- Beloborodov A.M., 1999, ApJ, 510, L123
- Coppi P., 1999, High Energy Processes in Accreting Black Holes, A.S.P. Conf. Ser. Vol. 161, Ed. Poutanen J., Svensson, R. p375
- Dolan J.F., 1992, ApJ, 384, 249
- Done C., Życki, P.T., 1999, MNRAS, 305, 457
- Done C., Mulchaey J.S., Mushotzky R.F., Arnaud K.A., 1992, ApJ, 395, 275
- Ebisawa K., Ueda Y., Inoue H., Tanaka Y., White N.E., 1996, ApJ, 467, 419

- Esin A.A., Narayan R., Cui W., Grove J.E., Zhang S.-N., 1998, *ApJ*, 505, 854
- Fabian A.C., Rees M.J., Stella L., White N.E., 1989, *MNRAS*, 238, 729
- Gierliński M., Zdziarski A.A., Done C., Johnson W.N., Ebisawa K., Ueda Y., Haard F., Philips B.F., 1997, *MNRAS*, 288, 958
- Gierliński M., Zdziarski A.A., Poutanen J., Coppi P.S., Ebisawa K., Johnson W.N., 1999, *MNRAS*, 309, 496
- Gies D.R., Bolton C.T., 1986. *ApJ*, 304, 371
- Marshall F.E., Mushotzky R.F., Petre R., Serlemitsos P.J., 1993, *ApJ*, 419, 301
- Massey P., Johnson K.E., DeGioia-Eastwood K., 1995, *ApJ*, 454, 151
- Nayakshin S., 2000, *ApJ*, 534, 718
- Nayakshin S., Kazanas D., Kallman T.R., 2000, *ApJ*, 537, 833
- Nowak M.A., Wilms J, Vaughan B.A., Dove J.B., Begelman M.C., 1999, *ApJ*, 515, 726
- Page D.N., Thorne K.S., 1974, *ApJ*, 191, 499
- Poutanen J., Coppi P.S., 1998, *Physica Scripta*, T77, 57 ([astro-ph/9711316](http://astro-ph/9711316))
- Ross R.R., Fabian A.C., 1993, *MNRAS*, 261, 74
- Ross R.R., Fabian A.C., Brandt W.N., 1996, *MNRAS*, 278, 1082
- Ross R.R., Fabian A.C., Young A.J., 1999, *MNRAS*, 306, 461
- Róžańska, A., 1999, *MNRAS*, 308, 751
- Tanaka Y., Lewin W.H.G., 1995, *X-ray Binaries*, Cambridge University Press
- Zdziarski A.A., Lubiński P., Smith D.A., 1999, *MNRAS*, 303, L11
- Zhang S.N., et al., 1997, *ApJ*, 477, L95

## APPENDIX A: BLURRING MODEL SPECTRA

The disc spectra are convolved with the kernel of the DISKLINE model (Fabian et al. 1989). In order to do this our disc spectrum must be evaluated outside the range over which we are fitting the data. This is because, for example, higher energy photons may be redshifted into the band we are fitting. If the response matrix of the detector is such that the set of channels that correspond to a higher energy photon is distinct from the set of channels channels that correspond to a photon in the energy range being fitted then the model will not be evaluated at that higher energy and hence that contribution will be lost. This leads to the model spectrum dropping off at the edges of the range being fitted.

A solution to this is to firstly combine the response and auxiliary response matrices, and to replace the auxiliary response matrix with one in which the effective area of each energy bin is unity. The EXTEND command may then be used to enlarge the energy range over which the model is evaluated. This solves the problem.